



Kumar Saurabh, Department of Engineering Science and Ocean Engineering, National Taiwan University, Taiwan (kumar.saurabh@gmail.com)

Advisor: Prof. Tony Wan-Henn Sheu, Prof. Maxim Solovchuk

GPU based simulation in COVID-19 E-protein, pentameric ion-channel

Abstract

Transport of ions across an ion channel can be examined using continuum approach based Poisson-Nernst-Planck (PNP) equations with the inclusion of non-ionic repulsion modeled using Lennard-Jones potential. For voltage-gated ion channels, potential difference across the channel acts as the trigger for gating. Once the channel is open, depending on the selectivity of the channel, ionic species start moving across it, thereby resulting in ionic current. Many experimental studies are based on recording current across one channel or multiple channels embedded in a lipid bilayer where the bath environment is controlled explicitly. These studies have been useful in determining properties of the channel such as its selectivity, current-voltage relation etc.

Problem description

PNP equations describe the transport of ions under the influence of electrochemical gradient. It is a nonlinear system which couples diffusion and electrostatics where the nonlinearity arises from the drift effect of electric field on the concentration of ions. PNP equations in conjunction with Lennard-Jones potential can be expressed through the system of equations given below

$$-\nabla \cdot (\epsilon_0 \epsilon_r \nabla \phi) = \sum_{i=1}^N z_i e c_i; \mathbf{J}_i = -D_i \nabla c_i - \frac{D_i c_i}{k_B T} z_i e \nabla \phi - \frac{D_i c_i}{k_B T} \sum_{j=1}^N g_{ij} \nabla c_j; i = 1, \dots, N-1$$

$$\frac{\partial c_i}{\partial t} + \nabla \cdot \mathbf{J}_i = 0; \mathbf{J}_N = -D_N \nabla c_N - \frac{D_N c_N}{k_B T} z_N e \nabla \phi - \frac{D_N c_N}{k_B T} \nabla V - \frac{D_N c_N}{k_B T} \sum_{j=1}^N g_{ij} \nabla c_j$$

We solve the system for ϕ (electrostatic potential) and c_i (concentration). J_i represents flux for the i^{th} ionic species.

Methodology

Lattice Boltzmann method (LBM) is a mesoscopic description of flow based on kinetic theory. Flow is described through density distribution functions f_α , α being the lattice direction. Continuum variables and distribution functions are related through moments of distribution function as shown below.

Poisson Equation

$$\phi = \sum_{\alpha} f_{\alpha}^P$$

$$f_{\alpha}^{eq} = w_{\alpha} \phi$$

Nernst-Planck Equation

$$c_i = \sum_{\alpha} f_{\alpha,i}^{NP}$$

$$f_{\alpha,i}^{eq} = w_{\alpha} c_i \left(1 + \frac{e_{\alpha} V_{eff}}{c_s^2} \right)$$

where c_s represents the velocity of sound and $V_{eff} = -D_i \frac{z_i e}{k_B T} \nabla \phi + \sum_{j=1}^N g_{ij} \nabla c_j$.

Further, to accurately implement no-flux boundary condition at the complex channel-protein interface, Immersed Boundary Method (IBM) was implemented using predictor-corrector methodology¹.

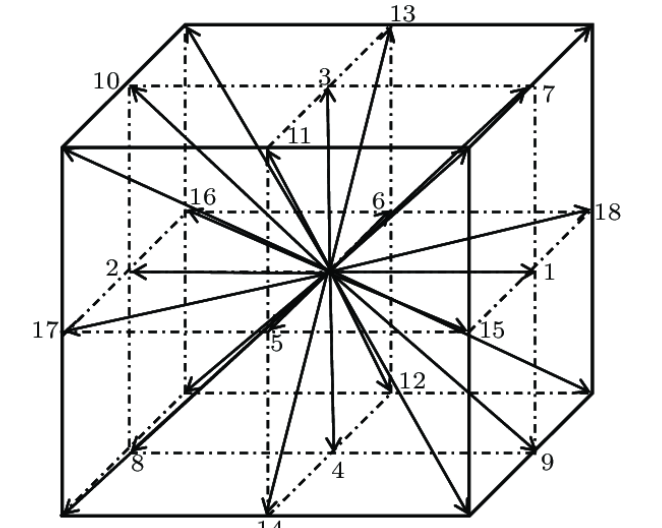


Figure 6: D3Q19 Lattice consisting of 19 Lattice directions.

Results

GPU Performance

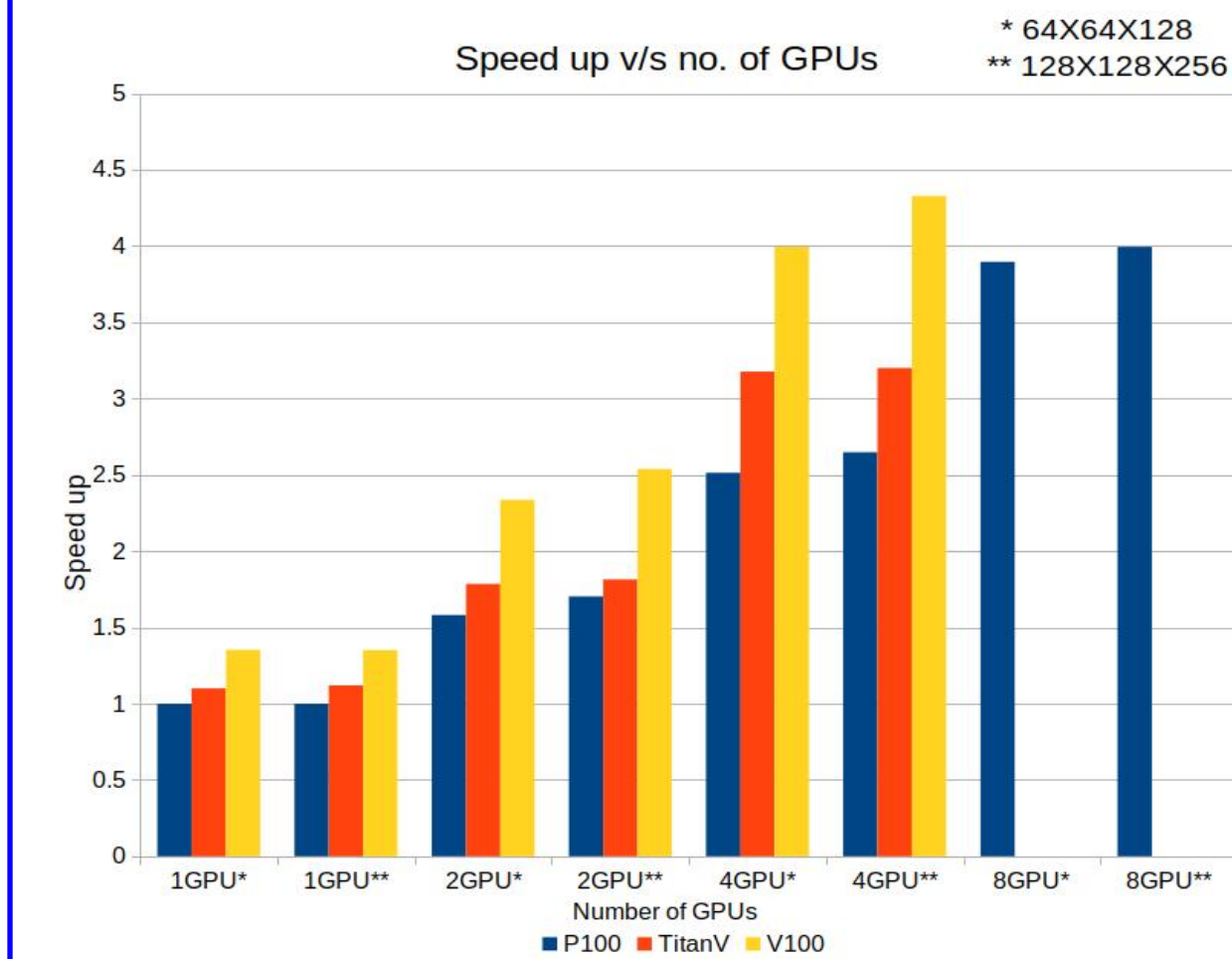


Figure 1: GPU performance comparison. V100 outperforms, P100 and Titan V. Addition of GPUs speeds up the calculation, maximum speedup observed for V100. Similar trend holds true for grid size as well. Increasing grid size increases overall time of computation, however performance gain upon adding more GPUs, is higher for larger grid size.

* time is in ms.

Concurrency

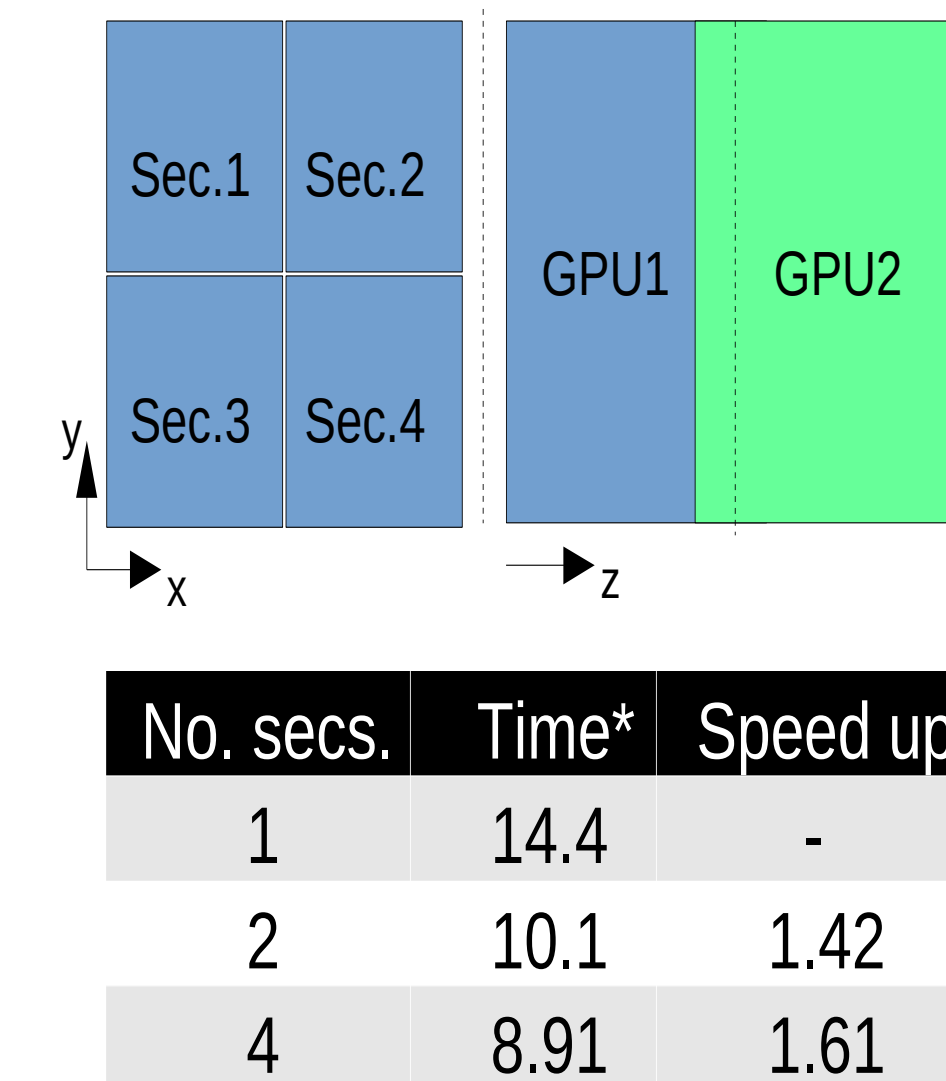


Figure 2: GPUs with multiple streams allow execution and transfer of data in parallel. To utilize it, we divided GPU domain into more sections such that GPU can perform the code execution in one domain while data transfer in the other. Upon introducing 2 and 4 sections for each GPU we observed a speed up of 1.42 and 1.61 respectively.

Data Restructuring

Array of Structures

0	...	18	...	0	...	18
X = 0	X = 0	X = Nx	X = Nx	Y = 0	Y = Ny	Y = Ny
Y = 0	Y = 0	Y = Ny	Y = Ny	Z = 0	Z = Nz	Z = Nz

Structure of Arrays

0	...	0	...	18	...	18
X = 0	X = Nx	X = 0	X = Nx	Y = 0	Y = Ny	Y = Ny
Y = 0	Y = Ny	Y = 0	Y = Ny	Z = 0	Z = Nz	Z = Nz

Array	Time*	Speed up
4D	14.4	-
AoS	7.57	1.91
SoA	6.37	2.26

Figure 3: Structures for storing data in LBM can also influence the performance of GPUs as different structures takes different time to access data while storing/reading. In our analysis we found out that AoS and SoA constructs provide a speed up of 1.91 and 2.26 over a regular 4D construct on a single GPU.

COVID-19

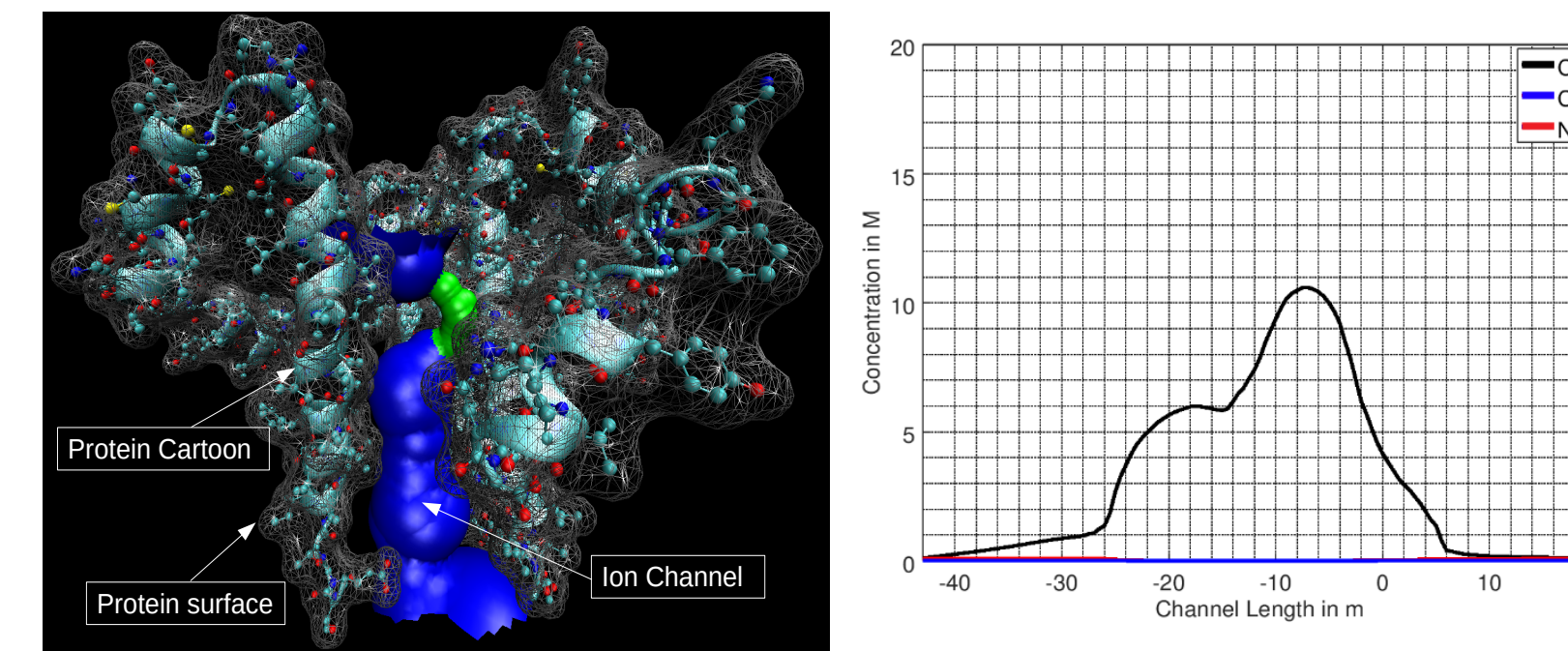


Figure 4: a) COVID-19, E protein, pentameric ion channel structure. b) Concentration distribution of Ca^{2+} , Na^{+} and Cl^{-} ions inside the ion channel. Results suggest that the ion channel is Chloride selective.

KcsA

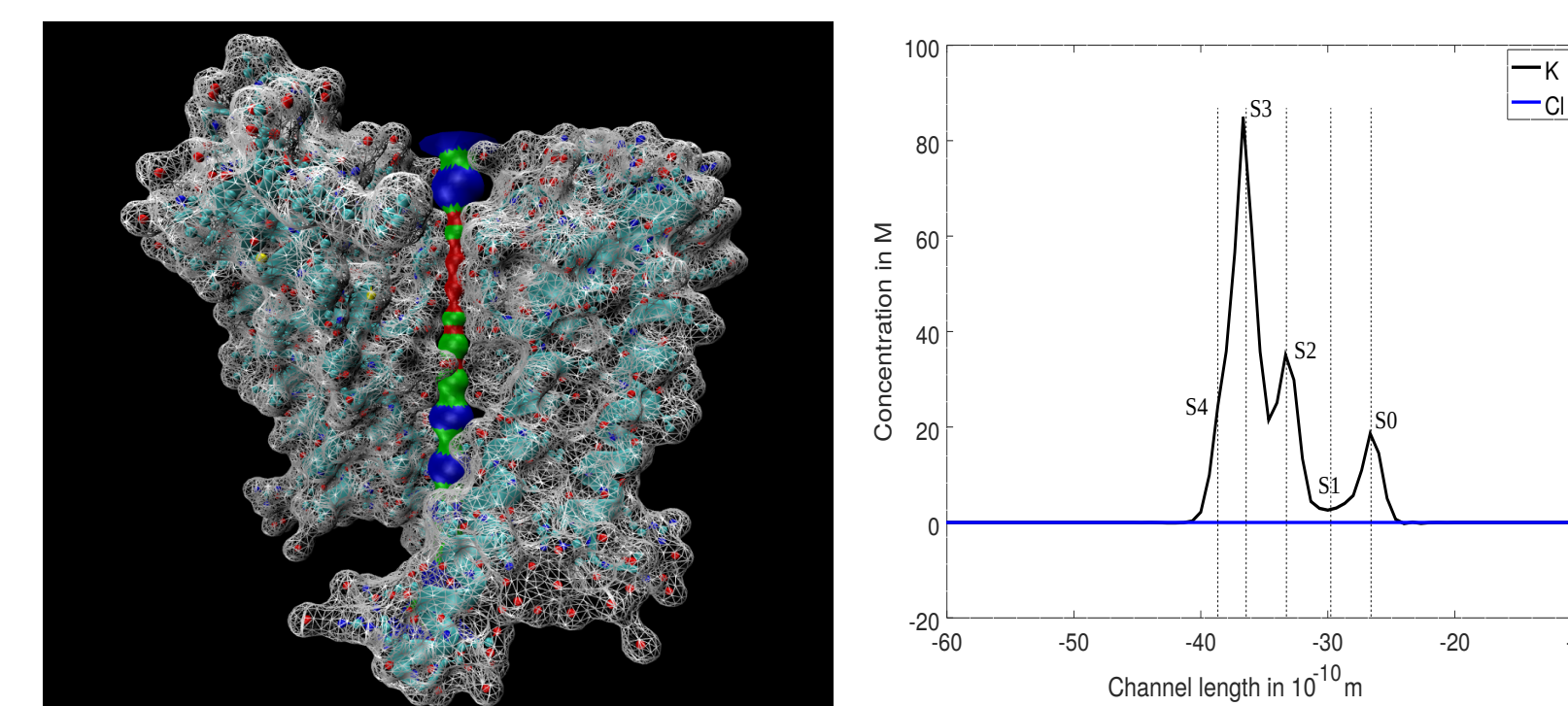


Figure 5: a) Potassium(KcsA) ion channel. b) Concentration distribution of K^{+} and Cl^{-} ions inside the ion channel. Results suggest that the ion channel is cation selective. Peaks in the concentration profiles coincide with binding sites S0-S4 for KcsA which are also observed in microscopic analysis like MD simulations etc.

Initial and Boundary Conditions

Ion concentrations and potential values are initialized at channel inlet and outlet and dirichlet boundary conditions are implemented there subsequently. No flux boundary condition is applied at channel-protein interface.

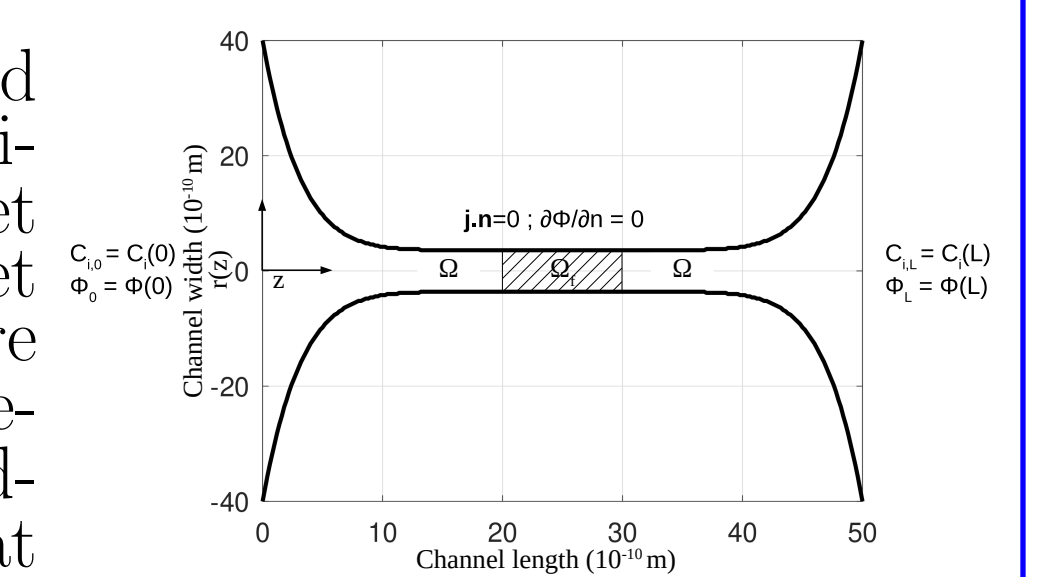


Figure 7: Schematic of a simple channel.

Acknowledgments

The work is supported

- Financially by NHRI and MOST
- Computer services by NCHC and NTU HPSCC
- Academic advices from Prof. Bob Eisenberg and Prof. Liu Jinn-Liang.

A special thanks to Dr. Shepard Shi (NCHC Director), Dr. Alpha Wang and Dr. Cesar Sun.

References

1. Saurabh, K., Solovchuk, M. A. and Sheu, T. W-H. Solution of Ion Channel Flow Using Immersed BoundaryLattice Boltzmann Methods. *J. Comp. Biol.*